

# An analysis of the impact of nanofluids on the cooling effectiveness of pin and perforated heat sinks

Taha Tuna Göksu<sup>1\*</sup>

<sup>1</sup>Adiyaman University, Mechanical Engineering Department, Türkiye

**Orcid:** T. T. Göksu (0000-0003-2028-3362)

**Abstract:** In the presented numerical study, the effect of the use of mono and hybrid (CuO/Water at 2% volume concentration and CuO + Fe/Water (1% CuO + 1% Fe)) type nanofluid in heat sinks designed in new geometric structures used to increase the processor cooling performance was investigated. The geometries used are circular, triangular, square, hexagonal, square, and hexagonal, and their perforated structures and their effects on a total of eight geometries were analyzed. In addition to these, the rate of improving the temperature distribution and heat transfer in the heat sink, i.e., the Performance Evaluation Criterion (PEC), was also examined. According to the results obtained, the lowest thermal resistance value is seen in the circular cross-section with  $R_{th} = 0.289$  K/W, while the highest thermal, i.e., cooling performance is seen in the triangular perforated structure with  $R_{th} = 0.63$  K/W and at the lowest pressure inlet condition. In terms of temperature distribution, the most uniform distribution was obtained between 311.82 and 308.98 K in the circular section. The most interesting result in terms of the results was the  $PEC = 1.4$  for the triangular hole structure in the heat transfer improvement performance. The main reason for this is that the range of the temperature distribution shown is very high (319–311.5K).

**Keywords:** heat sink, mono-hybrid nanofluid, PEC, thermal resistance

## 1. Introduction

Thermal problems in central processing unit (CPU) equipment need the use of passive cooling methods, such as pin or plate fin heat sinks (HS), to ensure effective heat transfer and cost efficiency [1–4]. The research conducted by Chiu et al. [5,6] examined the cooling effectiveness of pin-type HS with circular cross-sections using both computational and experimental approaches. HS performance is highly influenced by factors such as fin dimensions, forms, quantity, arrangement, heat surface placement, and coolant type. Göksu et al. [7,8] have obtained important results of heat transfer improvement by using passive methods, i.e., geometrical modifications, in their studies. Kuru [9] investigates the performance of triangular ribbed plate fin HS, focusing on their thermal efficiency, weight, volume, and cost reduction. The results show that increasing velocity, fin height, number of fins, and triangular rib height leads to lower pressure drop and increased HS volume and weight. Different manufacturing techniques also play an important role in the design of heat sinks; for example, pin-type geometry with addi-

tive manufacturing was designed and its effects analyzed [10]. Thangavel and Sekar [11] designed a lotus-type heat sink, analyzed the temperature distributions in laminar and turbulent flow, and observed that they decreased up to 302 K.

Nanofluids (NFs) are being used more and more to improve heat transfer in different HS setups because to their high thermal conductivity and density. The computational study conducted by Kavitha et al. [12] demonstrated a significant 68% enhancement in heat transfer for a fin-type HS by utilizing  $Al_2O_3$ /water nanofluid. Choi [13] initially introduced the notion of employing nanoparticles in coolant. Choi and Eastman [14] employed NFs to enhance thermal control in electronic applications. Wu et al. [15] investigated the use of  $Al_2O_3$ -water NF in copper microchannel HS, as well as graphene/water NF for cooling serpentine and sinusoidal spiral architectures in heat sinks. In a study, it was shown that the utilization of a sinusoidal winding fin design was more effective when combined with a graphene/water NF on HS that had serpentine and sinusoidal spiral designs [16].

\*Corresponding author:

Email: tgoksu@adiyaman.edu.tr

**Cite this article as:**

Göksu, T. T. (2024). An analysis of the impact of nanofluids on the cooling effectiveness of pin and perforated heat sinks. *European Mechanical Science*, 8(2): 71-77. <https://doi.org/10.26701/ems.1466806>

**History dates:**

Received: 08.04.2024, Revision Request: 24.04.2024, Last Revision Received: 30.04.2024, Accepted: 01.05.2024



© Author(s) 2024. This work is distributed under <https://creativecommons.org/licenses/by/4.0/>



An investigation was conducted on a mini-channel HS with a wavy design to assess its cooling performance using supercritical CO<sub>2</sub>. Results showed a significant 8.58-fold rise in the heat transfer coefficient at the lowest input temperature of 305 K [17]. The combination of wavy fins and square fins greatly enhances the performance of an inclined cooler box that contains magnetized-radiative NF, resulting in a notable improvement [18,19]. The utilization of NF-cooled fins with circular, square, and triangular shapes led to significant enhancements in the Nusselt number, with increases of 23.1%, 16.5%, and 8%, correspondingly [20]. The integration of the Eulerian-Lagrangian approach with NF results in a significant 16% improvement in the heat transfer coefficient of a micro pin-fin HS [21,22]. Cabir [23] and Uçkan et al. [24,25] are noteworthy in this regard in their studies on fuels.

Moreover, a study investigating the utilization of MgO/water, TiO<sub>2</sub>/water, and Al<sub>2</sub>O<sub>3</sub>/water, NFs in a rectangular microchannel HS revealed that Al<sub>2</sub>O<sub>3</sub>/water and MgO/water NFs yielded superior outcomes [26]. The study examines [27] the impact of nanoparticle morphology on thermal conductivity in microchannels, focusing on hybrid and mono NFs. Results show that Al<sub>2</sub>O<sub>3</sub> mono NF increases thermal conductivity by 12%, while hybrid NF based water increases it by 18.6%. TiO<sub>2</sub> nanoparticles have the highest thermal resistance. Ozbalcı et al. [28] conducted research indicating that the combination of nanofluids and metal foam is an economical and energy-efficient method for cooling electronic systems. Karaaslan and Menlik [29] conducted a study to examine the effects of mono and hybrid NFs on the cooling of solar panels. The mono-hybrid nanofluids they use are CuO/Water and CuO+Fe/Water. The reason for choosing these two fluid types is that the thermophysical properties of nanofluids are better, as mentioned above. The behavior of hybrid nanofluids can be more precisely estimated at lower concentrations of nanoparticles. Therefore, a concentration of 2% is deemed the most appropriate for this experiment [30]. In their study, Ho et al. [31] investigated the impact of ultrapure water and water-based alumina NFs with volume concentrations of 0.5% and 1% on a micro-channel HS. They observed a significant 14.43% enhancement in the heat transfer coefficient. Sriharan et al. [32] conducted a study to examine how the use of nanofluids Al<sub>2</sub>O<sub>3</sub>, MgO, and CuO affects the convective heat transfer coefficient in a HS with a hexagonal tube. The results indicated a significant increase of 40%, 28%, and 22% for Al<sub>2</sub>O<sub>3</sub>, MgO, and CuO, respectively.

Göksu [33] investigated the cooling performance of mono and hybrid NFs in block-type HS, and the results showed that mono NF provided much better thermal resistance than water fluid and partially lower thermal resistance than hybrid NF. It was observed that Al<sub>2</sub>O<sub>3</sub> NF provides lower thermal resistance than water fluid when used in block-type structures [34]. In another study, Göksu [35] designed heat sinks with circular, triangular, square, and hexagonal cross-sections and their perforated versions and investigated their cooling performance using water

fluid. The results showed that R<sub>th</sub> = 0.29 K/W had the lowest thermal resistance. The present study examined the effects of using mono and hybrid nanofluid instead of water in HS designed in circular, triangular, square, and hexagonal sections, as well as their perforated versions from the previous study. The primary driving force behind this examination was the impact of mono and hybrid nanofluids on block-type structures in a previous study, which raised questions about the cooling capabilities of pin and perforated pin structures. Within this framework, it will assess and contrast the cooling and heat transfer enhancements achieved by water, mono nanofluids, and hybrid nanofluids.

## 2. Geometry and Boundary Condition

The geometries used in the present study are the same as those used in the previous study [35]. These geometries are circular, triangular, square, square, hexagonal, and their perforated versions. Four different inlet pressures are used as boundary conditions (689, 1370, 2040, 2750 Pa), and a constant heat flux is applied to the bottom side of the heat sink. Central Processing Unit (CPU) analyses were carried out using the ANSYS FLUENT module. The k-ε turbulence module was used, and SIMPLE was selected as the solver. The residual stress values were kept the same as in the previous study. Equation 1 uses the thermal resistance (R<sub>th</sub>) as the fundamental parameter to gauge the system's cooling efficiency. The system cools more efficiently the lower this value is. Equations 2–5 display the heat transfer coefficient, friction factor, Reynolds number, and Performance Evaluation Criteria (PEC). The present study uses both mono (CuO/Water-2% concentration) and hybrid (CuO-1%+Fe/Water-1% concentration) solutions. The equations used in the calculation of the physical properties of the fluids are given in 6–13 equations [33].

$$R_{th} = \frac{T_{CPU,m} - T_{in}}{q''} \quad (1)$$

$$h = \frac{q''}{T_{CPU,m} - T_{bf,th}} \quad (2)$$

$$Re = \frac{\rho \cdot V \cdot D_h}{\mu} \quad (3)$$

$$f = \frac{2 \cdot \Delta P \cdot D_h}{\rho \cdot L \cdot V^2} \quad (4)$$

$$PEC = \frac{h_a/h_0}{(f_a/f_0)^{1/3}} \quad (5)$$

$$\rho_{nf} = \varphi \rho_p + (1 - \varphi) \rho_{bf} \quad (6)$$

$$\mu_{nf} = \frac{\mu_{bf}}{(1 - \varphi)^{2.5}} \quad (7)$$

$$\frac{k_{nf}}{k_{bf}} = \frac{3 \left( \frac{k_f}{k_{bf}} - \varphi \right)}{\left( \frac{k_f}{k_{bf}} + 2 \right) - \left( \frac{k_f}{k_{bf}} - 1 \right) \varphi} \quad (8)$$

$$(\rho C)_{nf} = \varphi_p \rho_p C_p + (1 - \varphi_p) \rho_{bf} C_{bf}. \tag{9}$$

$$\rho_{hnf} = \varphi_1 \rho_{p1} + \varphi_2 \rho_{p2} + (1 - (\varphi_1 + \varphi_2)) \rho_{bf}, \tag{10}$$

$$\mu_{hnf} = \mu_{bf} (1 + 32.795\varphi - 7214\varphi^2 + 714600\varphi^3 - 0.194110^8\varphi^4), \tag{11}$$

$$\frac{k_{nf}}{k_{bf}} = \left( \frac{1.747 \cdot 10^6 + \varphi_p}{1.747 \cdot 10^6 - 1.498 \cdot 10^6 \varphi_p + 1.117 \cdot 10^8 \varphi_p^2 + 1.997 \cdot 10^9 \varphi_p^3} \right), \tag{12}$$

$$(\rho C)_{hnf} = \varphi_{p1} \rho_{p1} C_{p1} + \varphi_{p2} \rho_{p2} C_{p2} + (1 - \varphi_{p1} - \varphi_{p2}) C_{bf}. \tag{13}$$

### 3. Result and Discussion

This chapter will be analyzed in three sections. The sections are categorized according to the fluids used, and the first one highlights the results of the previous study [35], i.e., when water fluid is used, the second one highlights the results when mono nanofluid is used, and the last section highlights the results when hybrid nanofluid is used. According to the numerical data, the highest flow rate shows a maximum deviation of 4.69% in  $R_{th}$ , while the maximum variation in  $\dot{V}$  is 6.42% at a pressure of 1370 Pa. These variations are worth mentioning as they are within the permissible range of less than 10%, which demonstrates the accuracy of the numerical simulations.

#### 3.1. Water Utilization Findings

The thermal resistance, temperature distribution, and PEC results obtained in the previous study [35] are shown in Figures 1, 2, and 3, respectively. As can be seen from the figures, the thermal resistance values decrease with increasing pressure, and the lowest thermal resistance was obtained as  $R_{th} = 0.29 \text{ K/W}$  at  $P = 2750 \text{ Pa}$ . It is clearly seen from the figure that the geometry that can be used in terms of cooling performance after the circular cross-sectional structure is the heat sink in the square hole structure. The specified value was obtained in the circular-section pin heat sink. In the temperature distribution, the situation is the same; that is, it is seen that the temperature decreases with increasing pressure, and the most uniform temperature distribution (311.3–308.73 K) was obtained in the circular section pin type heat sink. When the Performance Evaluation Criteria (PEC) were evaluated, the highest PEC = 1.18 was obtained at  $P = 689 \text{ Pa}$ . Another important result is that the heat sink with a triangular cross-sectional structure has the lowest PEC values.

#### 3.2. Mono-Nanofluid Utilization Findings

Figures 4, 5, and 6 display the thermal resistance, temperature distribution, and PEC results obtained using mono (CuO/Water, 2% concentration) nanofluid, respectively. The numerical results indicate that the heat sink in the circular cross-section has the lowest thermal resistance value of  $R_{th} = 0.289 \text{ K/W}$ . Overall, the circular cross-section yields better results than the other cross-sections. It is evident that the value is lower than that of water fluid. This finding is one of the most significant outcomes of using nanofluid to cool heat sinks. Among the

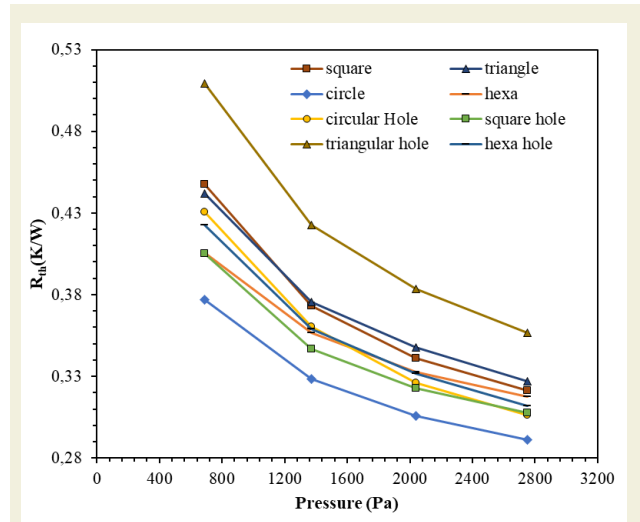


Figure 1. Compare of pressure vs. thermal resistance.

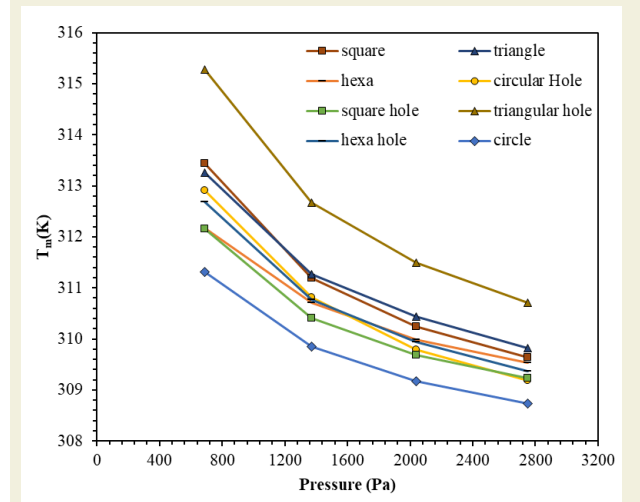


Figure 2. Mean temperature vs. pressure.

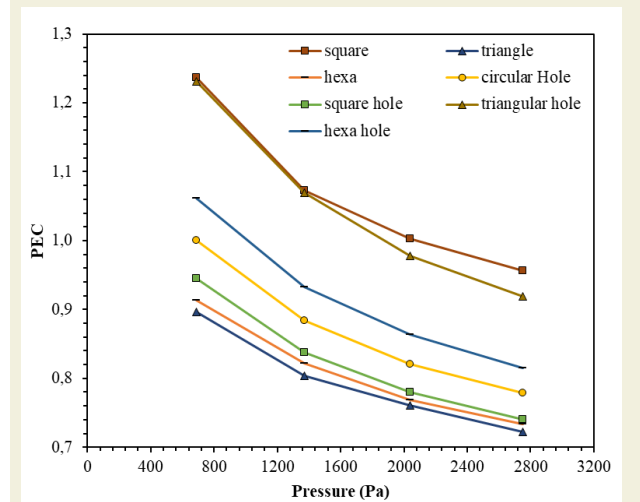


Figure 3. PEC vs. pressure drop.

perforated structures, the square hole structure exhibited the lowest thermal resistance, with  $R_{th} = 0.302 \text{ K/W}$ . The most uniform temperature distribution was achieved in the 311.34–308.67 K range, particularly in the circular section heat sink. This range is comparatively better than that achieved using water fluid. One of the key findings

of this study is the PEC value. As shown in Figure 6, the triangular hole structure at  $P = 689$  Pa yielded the highest PEC value of 1.32, which is significantly higher than the highest PEC value of 1.18 observed in water fluid. This indicates that the mono-nanofluid has a considerable

impact on PEC values compared to water fluid. From Figure 3, it is evident that the lowest PEC value of 0.71 was obtained when using mono nanofluid, compared to 0.67 when using water fluid.

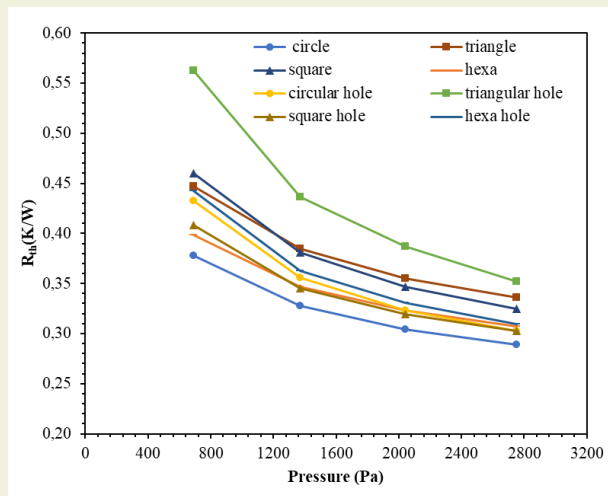


Figure 4. Compare of pressure vs. thermal resistance for mono nanofluid.

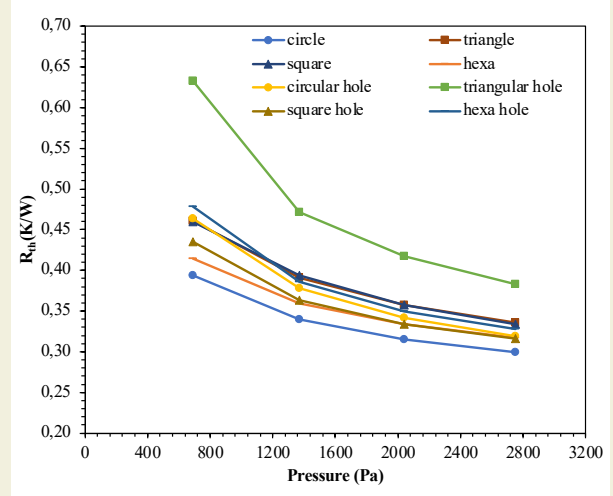


Figure 7. Compare of pressure vs. thermal resistance for hybrid nanofluid.

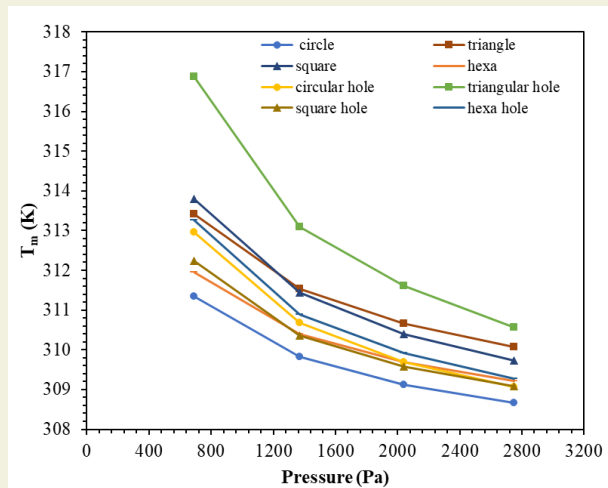


Figure 5. Mean temperature vs. pressure for mono nanofluid.

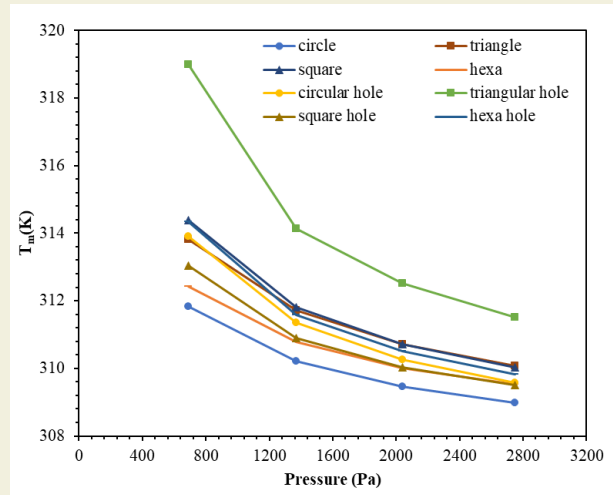


Figure 8. Mean temperature vs. pressure for hybrid nanofluid.

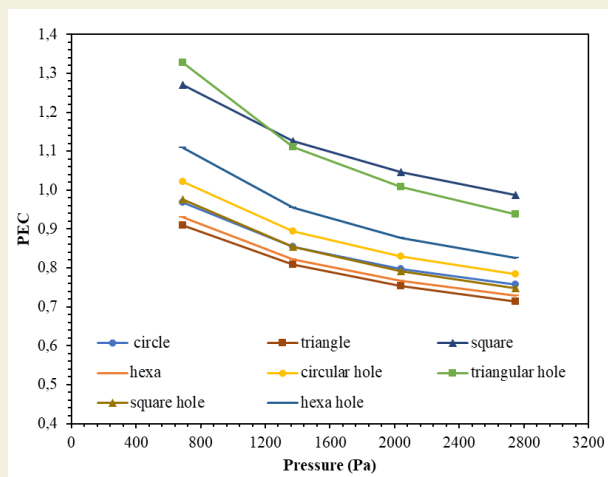


Figure 6. PEC vs. pressure drop for mono nanofluid.

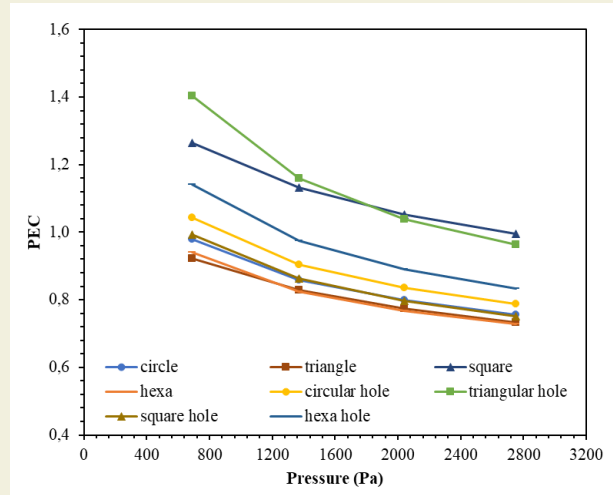


Figure 9. PEC vs. pressure drop for hybrid nanofluid.

### 3.3. Hybrid-Nanofluid Utilization Findings

Figures 7, 8, and 9 display the thermal resistance, temperature distribution, and PEC results obtained using mono (CuO+Fe/Water) nanofluid, respectively. The circular cross-section heat sink exhibited the lowest thermal resistance and the most uniform temperature distribution, with values of  $R_{th} = 0.299$  K/W and 311.82–308.98 K, respectively. These values are higher than those of the mono nanofluid. The study concludes that the hybrid nanofluid is not more efficient than the mono nanofluid in terms of thermal resistance and temperature distribution. However, it is quite efficient in terms of heat enhancement factor (PEC). Figure 9 shows that the maximum PEC is 1.32 in the mono nanofluid, while it is 1.40 in the hybrid nanofluid. Although the lowest PEC value in mono nanofluid is 0.67, the value of 0.733 in hybrid nanofluid indicates its superior efficiency in terms of heat recovery.

## 4. Conclusion

The key findings regarding the cooling, temperature distribution, and heat recovery performances of mono and hybrid nanofluids in the heat sink are as follows:

1. The heat resistance of the mono nanofluid was reduced compared to both the water fluid and the hybrid nanofluid. The circular sectioned heat sink achieved the lowest thermal resistance, with a value of  $R_{th}=0.289$  K/W.
2. The evaluation of temperature distribution indicated that the mono nanofluid exhibited a more consistent temperature distribution compared to the hybrid and water fluids.
3. The temperature distribution was obtained in the range of approximately 311-308 K for both mono and hybrid nanofluids. This range's narrowness is an indication of how uniform the temperature distribution is.
4. Upon comparing the results in terms of PEC, it was seen that the hybrid nanofluid exhibited much higher values compared to both the mono nanofluid and water fluid. The heat sink with triangular holes achieved the greatest PEC value of 1.40. The impact of perforated structures, particularly in PEC outcomes, serves as the fundamental measure of the effectiveness of the planned geometries.

## Nomenclature

$a$	results parameter of specified study
$C_p$	specific heat, $J.kg^{-1}.K^{-1}$

$D_h$	hydraulic diameter, m
$f$	friction factor
$h$	convection heat transfer coefficient, $W.m^{-2}.K^{-1}$
$k$	thermal conductivity, $W.m^{-1}.K^{-1}$
$q''$	heat flux, $W.m^{-2}$
$R_{th}$	effective thermal resistance $K.W^{-1}$
$T$	temperature, K

## Greeks

$\mu$	dynamic viscosity, Pa·s
$\rho$	density, $kg.m^{-3}$
$0$	results parameters of experimental study

## Abbreviations

CFD	computational fluid dynamics
CPU	central processing unit
HS	heat sink
NF	nanofluid
PEC	performance evaluation criterion

## Research Ethics

Ethical approval not required.

## Author Contributions

The author(s) accept full responsibility for the content of this article and have approved its submission.

## Competing Interests

The author(s) declare that there are no competing interests.

## Research Funding

Not reported.

## Data Availability

Not applicable.

## References

- [1] Ajayan, J., Nirmal, D., Tayal, S., Bhattacharya, S., Arivazhagan, L., Fletcher, A. A., & Ajitha, D. (2021). Nanosheet field effect tran-

sistors-A next generation device to keep Moore's law alive: An intensive study. *Microelectronics Journal*, 114: 105141. <https://doi.org/10.26701/ems.1466806>

- doi.org/10.1016/j.mejo.2021.105141.
- [2] Matallana, A., Ibarra, E., López, I., Andreu, J., Garate, J. I., Jordà, X., & Rebollo, J. (2019). Power module electronics in HEV/EV applications: New trends in wide-bandgap semiconductor technologies and design aspects. *Renewable and Sustainable Energy Reviews*, 113, 109264. <https://doi.org/10.1016/j.rser.2019.109264>.
  - [3] Jayaramu, P., Gedupudi, S., & Das, S. K. (2021). Experimental investigation of the influence of boiling-induced ageing on high heat flux flow boiling in a copper microchannel. *International Journal of Heat and Mass Transfer*, 181, 121862. <https://doi.org/10.1016/j.ijheatmasstransfer.2021.121862>.
  - [4] Al-Neama, A. F., Kapur, N., Summers, J., & Thompson, H. M. (2018). Thermal management of GaN HEMT devices using serpentine minichannel heat sinks. *Applied Thermal Engineering*, 140, 622-636. <https://doi.org/10.1016/j.applthermaleng.2018.05.072>.
  - [5] Chiu, H. C., Hsieh, R. H., Wang, K., Jang, J. H., & Yu, C. R. (2017). The heat transfer characteristics of liquid cooling heat sink with micro pin fins. *International communications in heat and mass transfer*, 86, 174-180. <https://doi.org/10.1016/j.icheatmasstransfer.2017.05.027>.
  - [6] Chiu, H. C., Youh, M. J., Hsieh, R. H., Jang, J. H., & Kumar, B. (2023). Numerical investigation on the temperature uniformity of micro-pin-fin heat sinks with variable density arrangement. *Case Studies in Thermal Engineering*, 44, 102853. <https://doi.org/10.1016/j.csite.2023.102853>.
  - [7] Göksu, T. T., & Yılmaz, F. (2021). Numerical comparison study on heat transfer enhancement of different cross-section wire coils insert with varying pitches in a duct. *Journal of Thermal Engineering*, 7(7), 1683-1693. <https://doi.org/10.18186/thermal.1025930>.
  - [8] Yılmaz, İ. H., & Göksu, T. T. (2019). Enhancement of heat transfer using twisted tape insert in a plain tube. *Bitlis Eren Üniversitesi Fen Bilimleri Dergisi*, 8(1): 251-260. <https://doi.org/10.17798/bitlisfen.462169>.
  - [9] Kuru, M. N. (2023). The effect of the triangular rib usage in the plate fin heat sinks on the pressure drop, base plate temperature, and entropy generation. *European Mechanical Science*, 7(2), 99-108. <https://doi.org/10.26701/ems.1276575>.
  - [10] Parlak, M. (2024). Thermal management with double layered heat sink produced by direct metal laser sintering. *International Journal of Energy Studies*, 9(1): 155-173. <https://doi.org/10.58559/ijes.1439889>.
  - [11] Thangavel, P., & SEKAR, A. (2021). Investigations on Heat Transfer Characteristics of Porous type Copper Heat Sink with Bifurcations. *Journal of Thermal Engineering*, 7(3): 584-594. <https://doi.org/10.18186/thermal.888428>.
  - [12] Mukeshkumar, P. C., & Kumar, A. (2023). Numerical study on the performance of Al<sub>2</sub>O<sub>3</sub>/water nanofluids as a coolant in the fin channel heat sink for an electronic device cooling. *Materials Today: Proceedings*. <https://doi.org/10.1016/j.matpr.2023.02.337>.
  - [13] Siginer, D. A., & Wang, H. P. (1995). Developments and Applications of Non-Newtonian Flows, 1995: Presented at the 1995 ASME International Mechanical Engineering Congress and Exposition, November 12-17, 1995, San Francisco, California.
  - [14] Choi, S. U., & Eastman, J. A. (1995). *Enhancing thermal conductivity of fluids with nanoparticles* (No. ANL/MSD/CP-84938; CONF-951135-29). Argonne National Lab.(ANL), Argonne, IL (United States).
  - [15] Wu, X., Wu, H., & Cheng, P. (2009). Pressure drop and heat transfer of Al<sub>2</sub>O<sub>3</sub>-H<sub>2</sub>O nanofluids through silicon microchannels. *Journal of Micromechanics and Microengineering*, 19, 105020. <https://doi.org/10.1088/0960-1317/19/10/105020>.
  - [16] Ghadikolaie, S. S., Siahchrehghadikolaie, S., Gholinia, M., & Rahimi, M. (2023). A CFD modeling of heat transfer between CGNPs/H<sub>2</sub>O Eco-friendly nanofluid and the novel nature-based designs heat sink: Hybrid passive techniques for CPU cooling. *Thermal Science and Engineering Progress*, 37, 101604. <https://doi.org/10.1016/j.tsep.2022.101604>.
  - [17] Khoshvaght-Aliabadi, M., Ghodrati, P., Mortazavi, H., & Kang, Y. T. (2023). Numerical analysis of heat transfer and flow characteristics of supercritical CO<sub>2</sub>-cooled wavy mini-channel heat sinks. *Applied Thermal Engineering*, 226, 120307. <https://doi.org/10.1016/j.applthermaleng.2023.120307>.
  - [18] Massoudi, M. D., & Hamida, M. B. B. (2023). Combined impacts of square fins fitted wavy wings and micropolar magnetized-radiative nanofluid on the heat sink performance. *Journal of Magnetism and Magnetic Materials*, 574, 170655. <https://doi.org/10.1016/j.jmmm.2023.170655>.
  - [19] Seyf, H. R., & Feizbakhshi, M. (2012). Computational analysis of nanofluid effects on convective heat transfer enhancement of micro-pin-fin heat sinks. *International Journal of Thermal Sciences*, 58, 168-179. <https://doi.org/10.1016/j.ijthermalsci.2012.02.018>.
  - [20] Ambreen, T., Saleem, A., & Park, C. W. (2019). Pin-fin shape-dependent heat transfer and fluid flow characteristics of water-and nanofluid-cooled micropin-fin heat sinks: Square, circular and triangular fin cross-sections. *Applied Thermal Engineering*, 158, 113781. <https://doi.org/10.1016/j.applthermaleng.2019.113781>.
  - [21] Cai, W., Toghraie, D., Shahsavar, A., Barnoon, P., Khan, A., Beni, M. H., & Jam, J. E. (2021). Eulerian-Lagrangian investigation of nanoparticle migration in the heat sink by considering different block shape effects. *Applied Thermal Engineering*, 199, 117593. <https://doi.org/10.1016/j.applthermaleng.2021.117593>.
  - [22] Yasir, M., Khan, M., Alqahtani, A. S., & Malik, M. Y. (2023). Numerical study of axisymmetric hybrid nanofluid MgO-Ag/H<sub>2</sub>O flow with non-uniform heat source/sink. *Alexandria Engineering Journal*, 75, 439-446. <https://doi.org/10.1016/j.aej.2023.05.062>.
  - [23] Cabir, B., & Yakın, A. (2024). Evaluation of gasoline-phthalocyanines fuel blends in terms of engine performance and emissions in gasoline engines. *Journal of the Energy Institute*, 112, 101483. <https://doi.org/10.1016/j.joei.2023.101483>.
  - [24] Uçkan, İ., Yakın, A., & Behçet, R. (2024). Second law analysis of an internal combustion engine for different fuels consisting of NaBH<sub>4</sub>, ethanol and methanol mixtures. *International Journal of Hydrogen Energy*, 49, 1257-1267. <https://doi.org/10.1016/j.ijhydene.2023.10.302>.
  - [25] Uçkan, İ., Yakın, A., & Behçet, R. (2024). Investigation of the effect of dead-state temperature on the performance of boron-added fuels and different fuels used in an internal combustion engine. *Heat Transfer Research*, 55(12). <https://doi.org/10.1615/HeatTransRes.2024050089>.
  - [26] Mukherjee, S., Wciślik, S., Khadanga, V., & Mishra, P. C. (2023). Influence of nanofluids on the thermal performance and entropy generation of varied geometry microchannel heat sink. *Case Studies in Thermal Engineering*, 49, 103241. <https://doi.org/10.1016/j.csite.2023.103241>.

- g/10.1016/j.csite.2023.103241.
- [27] Al-Fatlawi, A. W., & Niazmand, H. (2024). Thermal analysis of hybrid nanofluids inside a microchannel heat exchanger for electronic cooling. *Journal of Thermal Analysis and Calorimetry*, 149, 4119-4131. <https://doi.org/10.1007/s10973-024-12991-2>.
- [28] Ozbalci, O., Dogan, A., & Asilturk, M. (2023). Performance of discretely mounted metal foam heat sinks in a channel with nanofluid. *Applied Thermal Engineering*, 235, 121375. <https://doi.org/10.1016/j.applthermaleng.2023.121375>.
- [29] Karaaslan, I., & Menlik, T. (2021). Numerical study of a photovoltaic thermal (PV/T) system using mono and hybrid nanofluid. *Solar Energy*, 224, 1260-1270. <https://doi.org/10.1016/j.solener.2021.06.072>.
- [30] Martin, K., Sözen, A., Çiftçi, E., & Ali, H. M. (2020). An experimental investigation on aqueous Fe–CuO hybrid nanofluid usage in a plain heat pipe. *International Journal of Thermophysics*, 41, 1-21. <https://doi.org/10.1007/s10765-020-02716-6>.
- [31] Ho, C. J., Peng, J. K., Yang, T. F., Rashidi, S., & Yan, W. M. (2023). On the assessment of the thermal performance of microchannel heat sink with nanofluid. *International Journal of Heat and Mass Transfer*, 201, 123572. <https://doi.org/10.1016/j.ijheatmasstransfer.2022.123572>.
- [32] Sriharan, G., Harikrishnan, S., & Oztop, H. F. (2022). Performance improvement of the mini hexagonal tube heat sink using nanofluids. *Thermal Science and Engineering Progress*, 34, 101390. <https://doi.org/10.1016/j.tsep.2022.101390>.
- [33] Göksu, T. T. (2024). Enhancing cooling efficiency: Innovative geometric designs and mono-hybrid nanofluid applications in heat sinks. *Case Studies in Thermal Engineering*, 104096. <https://doi.org/10.1016/j.csite.2024.104096>.
- [34] Göksu, T. T. (2024) Numerical investigation of the cooling effect of Al<sub>2</sub>O<sub>3</sub> nanofluid in heat sinks. *All Sciences Academy*, 1277–1284.
- [35] Göksu, T. T. (2024). Investigation of pin and perforated heat-sink cooling efficiency and temperature distribution. *Journal of Thermal Analysis and Calorimetry*, 1-13. <https://doi.org/10.1007/s10973-024-13078-8>.